Nanoscale

PAPER

View Article Online
View Journal

Cite this: DOI: 10.1039/c5nr07496g

Actively targeted gold nanoparticles as novel radiosensitizer agents: an *in vivo* head and neck cancer model

Aron Popovtzer,*†[a,c] Aviram Mizrachi,†[a,c] Menachem Motiei,[b] Dimitri Bragilovski,[a] Leon Lubimov,[a] Mattan Levi,[c] Ohad Hilly,[a] Irit Ben-Aharon[a,c] and Rachela Popovtzer[b]

A major problem in the treatment of head and neck cancer today is the resistance of tumors to traditional radiation therapy, which results in 40% local failure, despite aggressive treatment. The main objective of this study was to develop a technique which will overcome tumor radioresistance by increasing the radiation absorbed in the tumor using cetuximab targeted gold nanoparticles (GNPs), in clinically relevant energies and radiation dosage. In addition, we have investigated the biological mechanisms underlying tumor shrinkage and the *in vivo* toxicity of GNP. The results showed that targeted GNP enhanced the radiation effect and had a significant impact on tumor growth ($P < 0.001$). The mechanism of radiation enhancement was found to be related to earlier and greater apoptosis (TUNEL assay), angiogenesis inhibition (by CD34 level) and diminished repair mechanism (PCNA staining). Additionally, GNPs have been proven to be safe as no evidence of toxicity has been observed.

Received 27th October 2015,
Accepted 15th December 2015

DOI: 10.1039/c5nr07496g

www.rsc.org/nanoscale

Introduction

Advances in radiation techniques combined with chemotherapy have changed the treatment paradigm of head and neck cancer, leading to a significant improvement in patient quality of life. However, local failure remains a significant problem with a 40 percent failure rate despite aggressive treatment. The main etiologies for tumor resistance and unresponsiveness are hypoxia, repopulation, and resistant cancer stem cells. Strategies to overcome these factors, although theoretically promising, have not proven effective in phase III studies.[1] Lately several studies have suggested that the administration of gold nanoparticles (GNP) into tumors may improve radiosensitivity.

Gold has been recognized since the 1950s as a biologically safe material,[2,3] with high flexibility in terms of particle size, shape, and functional groups for coating and targeting. GNPs have a wide range of theoretical and practical applications in medicine in general and in cancer therapy in particular, as drug carriers, photothermal agents, imaging contrast agents, and radiosensitizers. Additionally, their unique physiochemical surface properties, which allow them to be conjugated, by simple chemistry, to various peptides, proteins, antibodies, and other biomolecules, make GNPs ideal candidates to be used as targeted cancer biomarkers.[1,4,5] As a result, there has been substantial research into the *in vivo* chemical stability,[6–8] pharmacokinetics,[7] biodistribution,[8–13] and biotoxicity[7,9,14–17] of GNPs.

GNPs are ideal candidates to be used as radiosensitizing agents since high atomic number (Z) materials, such as gold ($Z = 79$) increase radiation sensitivity owing to their greater absorption of photons and release of secondary energy in the form of photoelectrons, auger electrons, and X-rays into surrounding tissue.[18,19] Therefore, the close proximity of GNP to nuclear DNA increases the probability of creating DNA strand breaks, the primary mechanism of radiation-induced cytotoxicity.[20,21] When GNPs specifically target cancer cells (*e.g. via* antibody–antigen interaction), large amounts of gold atoms accumulate in the tumor, leading to enhancement of the radiation effect on the tumor. However, there is unclarity regarding the mechanism underlying cell death. The main suggested hypothesis include increased apoptosis, increased generation of intracellular reactive oxygen species or direct DNA damage causing DNA double strand break.[20]

Several *in vitro*[2–4] and *in vivo*[5–8] studies have shown that increasing the absorption of radiation may have important clinical implications in terms of tumor shrinkage and prolonged survival. The main goals of our present study were (1) to determine whether cetuximab coated GNP, when under-

[a]*Head and Neck Cancer Radiation Clinic, Institute of Oncology, Davidoff Cancer Center, Rabin Medical Center, Petach Tikva 49100, Israel.*
E-mail: aronp@clalit.org.il
[b]*Faculty of Engineering & The Institute of Nanotechnology and Advanced Materials, Bar-Ilan University, Ramat Gan 5290002, Israel*
[c]*Sackler Faculty of Medicine, Tel-Aviv University, Ramat Aviv, Israel*
† Both authors contribute equally to this work.

going clinically relevant radiation treatment, have an effective radiosensitizing effect on HNSCC; (2) to investigate the biological mechanisms underlying tumor shrinkage, and (3) to investigate the *in vivo* toxicity of GNP.

Materials and methods

Induction of subcutaneous tumors

All animal experiments were carried out in compliance with the Israel Council on Animal Care regulations and were approved by the Animal Care Committee of the University Health Network. A431 cells (2 × 106) were injected subcutaneously into the back flank area of 36 nude mice aged 10–11 weeks. Tumor volume was measured by visualization for up to 6 weeks after treatment and by computed tomography (CT) at the end of the treatment. When the tumor reached a diameter of 8–10 mm, the mice were divided into 6 equal groups and randomly allocated for treatment with radiation, cetuximab (CTX) or GNP, alone and in various combinations; one group was untreated and served as a control.

Synthesis and characterization of GNP

The initial size and shape of the GNPs were chosen according to a previous study in which CTX-coated GNPs were used as contrast agents to improve CT imaging in head and neck cancer.[2] GNPs were prepared using sodium citrate, as described by Enustun and Turkevich.[14] Final particle size, shape, and uniformity were confirmed with a transmission electron microscope (TEM; JEM-1400, JEOL, Peabody, MA, USA). A protective layer of polyethylene-glycol (PEG) was incorporated onto the surface to reduce nonspecific interactions and prolong the circulation time of the particles in the bloodstream.[15] The PEG layer consisted of a mixture of thiol–polyethylene-glycol (HS-PEG–COOH) (~85%, MW ~ 5 kDa) and a heterofunctional polyethylene-glycol (HO-PEG–COOH) (~15%, MW ~ 3.4 kDa) (Creative PEGWorks, Winston Salem, NC, USA). For cancer cell targeting, the heterofunctional PEG was covalently conjugated to a CTX monoclonal antibody (Erbitux®, Merck KGaA, Darmstadt, Germany), and as a negative control, to an anti-rabbit IgG antibody (Jackson ImmunoResearch, West Grove, PA, USA), using 1-ethyl-3-(3′-(dimethylamino)propyl)-carbodiimide (EDC) and *N*-hydroxysulfosuccinimide (Sulfo-NHS) (Thermo Scientific, Waltham, MA, USA).[16,17]

GNP characterization

Samples were prepared by drop-casting 5 μL of the GNP solution onto standard carbon-coated film on a Cooper grid and then left to dry in a vacuum machine. The GNPs were further characterized at each stage using ultraviolet-visible spectroscopy (UV-1650 PC; Shimadzu, Kyoto, Japan) and measurement of the zeta potential (ZetaSizer 3000HS, Malvern Instruments, Worcestershire, UK). IgG or CTX coating (200 μL; 25 mg mL^{-1} Au) was performed 12 hours before the experiment, and the GNPs were administered to the test animals by injection into the tail vein.

Stereotactic radiation

The mice were anesthetized, and X-ray irradiation was performed using a Varian linear accelerator (True Beam); the 6 MV flattening filter-free mode was chosen so the treatment could be delivered as quickly as possible (1.4 Gy per minute). The dose was administered to the measured depth. A customized bolus of 1 cm was designed for each mouse to ensure skin coverage, calculated according to the depth of each tumor. The field size was determined according to the tumor size (from 1.5 × 1.5 to 2.0 × 2.0). Radiation was administered as a single fraction of 25 Gy.

Cetuximab

Cetuximab, alone or with radiation, was administered at a dose of 1 mg, as suggested in prior studies.[22]

Study design

The mice (36 mice total) were divided into 6 groups (6 mice per group). In order to measure the contribution of each factor of the experiment (radiation, cetuximab, targeted and non-targeted GNP) to the treatment outcome, each component has been examined separately (see Fig. 1).

All experiments were performed under general anesthesia. The mice were treated 10–11 days after SCC implementation, when the tumor size reached a diameter of 10 mm. To ensure a standardized tumor size at the time of treatment, size was defined by the calculated volume using the largest tumor diameters.

Group 1 served as untreated controls; group 2 received radiation only; group 3, CTX only; group 4, radiation + CTX; group 5, radiation + IgG-coated (non-targeted) GNP; and group 6 received radiation + CTX-coated (targeted) GNP. In groups 5 and 6, radiation (single fraction of 25 Gy) was administered 24 hours after injection of GNP (the time during which the nanoparticles accumulate in high density on the tumor). In

Groups*	Type of treatment
Group 1	Control (no treatment)
Group 2	Radiation
Group 3	CTX
Group 4	Radiation + CTX
Group 5	Radiation + IgG-GNP
Group 6	Radiation + CTX-GNP

Fig. 1 Summary table of mice experiments. CTX = cetuximab. *Each group contained 6 mice.

groups 2 and 4, the administration of radiation was timed to coincide with radiation treatment in groups 5 and 6.

Immunohistochemistry and confocal microscopy

To evaluate the histological effect of radiation, biopsy samples containing the tumor and adjacent tissue were taken from 2 mice in each treatment group at 1 and 6 weeks post treatment and further processed for histological analysis. Sections of fixed, paraffinized tumors and adjacent tissue were processed and incubated with primary antibodies: rabbit anti-Ki-67 (1 : 300; E1871; Spring Bioscience, CA, USA), rabbit anti-proliferating cell nuclear antigen (PCNA; 1 : 30; sc-7907; Santa Cruz Biotechnology) or rat anti-CD34 (1 : 200; CL8927AP, Cedarlane, Ontario, Canada). HRP-conjugated donkey anti-rabbit secondary antibody was used for immunoperoxidase Ki-67 staining. For immunofluorescence staining we used the following secondary antibodies: Alexa-555 conjugated goat anti-rat (1 : 400; Cell signaling technology, MA, USA) for CD34 staining and Alexa-488 conjugated donkey anti-rabbit (1 : 200; ab150065; Abcam, Cambridge, MA, USA) for PCNA staining. DNA was stained by Hoechst 33280 (1 μg ml^{-1}; Sigma). Images were obtained by using a LSM-510 confocal laser-scanning microscope (CLSM; Carl Zeiss MicroImaging, Oberkochen, Germany). Staining with secondary antibodies only served as negative control for immunofluorescence staining and was used for the photomultiplier offset calibration. Proliferation was assessed by quantification of Ki-67 positive cells per transverse section of the tumor.

Apoptosis evaluation

DNA fragmentation was examined *in situ* on paraffin-embedded tumor sections in mice by terminal transferase-mediated dUTP nick-end labeling (TUNEL; DeadEnd fluorometric TUNEL system, Promega, Madison, WI, USA) according to manufacturer's instructions. Sections exposed for 10 minutes to DNase I (6 units per ml; Invitrogen, Carlsbad, CA, USA) served as positive controls.

Apoptosis was assessed by TUNEL positive cells per transverse section of the tumor and adjacent tissue.

Statistical analysis

At least 20 transverse sections from each treatment group were examined for each stain. All tumor and adjacent tissue sections were analyzed. Representative images of hematoxylin and eosin (H&E), Ki-67, PCNA, CD34 and TUNEL-positive tumor sections are presented.

Toxicity evaluation

To evaluate GNP toxicity, blood was collected before, one week after, and 4 weeks after injection for analysis of complete blood count, liver function, and renal function. In addition, liver and kidney specimens were sent for histological examination of possible pathological changes. The organs were fixed in 10% neutral buffered formalin (~4% formaldehyde solution), and a cross-section from each was taken. The tissues were then trimmed, embedded in paraffin, sectioned at approximately 5-micron thickness, and stained with hematoxylin and eosin (H&E). All slides were examined by an experienced veterinary pathologist. Histological changes were graded from 0 (no change) to 3 (severe changes). The mice were also followed for behavioral signs of toxicity (stress and weight loss).

Results

GNP characterization

On TEM, the GNP appeared as uniformly distributed spheres of 30 nm diameter (Fig. 2A). An expanded signal on ultraviolet-visible spectroscopy and zeta potential results confirmed the chemical coating after each layer was completed (Fig. 2B and C). Maintenance of the same plasmon resonance for 3 months confirmed the continued stability of the control antibody-conjugated GNP.

Tumor volume

Tumor volumes in the mouse groups at 5 weeks after radiation treatment are shown in Fig. 3, and the average changes during this time are shown in Fig. 4. Groups 1–5 showed progression of tumor growth with time; in group 6 (radiation + CTX-GNP), the disease remained stable. The size of the largest diameter of the tumor (average for each group) in the first and last measurements for each group were: group 1: 1.1 to 2.1 cm; group 2: 1.1 to 1.4 cm; group 3: 1.1 to 2 cm; group 4: 1.5 to

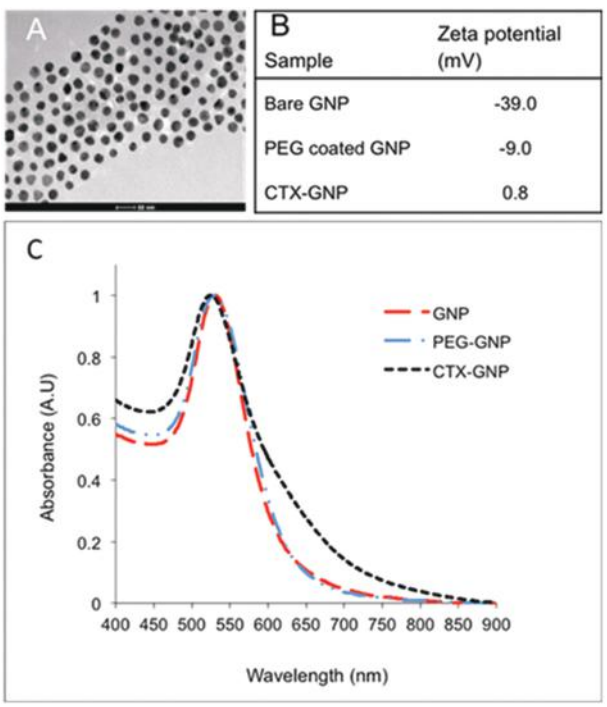

Fig. 2 Characterization of GNP. A: TEM image of 30 nm GNP. B: Zeta potential measurements. C: UV-vis spectroscopy of the bare GNP, PEGylated GNP, CTX-GNP.

Group No.	Type of treatment	Tumor volume (cm^3) differential average	*P* value (t test)
1	Control	+1.03	Ref.
2	Radiation	+0.4	0.106
3	CTX	+0.83	0.649
4	Radiation+CTX	+0.3	0.055
5	Radiation+IgG-GNP	+0.57	0.419
6	Radiation+CTX-GNP	0	0.001

Fig. 3 Average changes in tumor volume for each mouse group over 5 weeks after radiation. GNPs = gold nanoparticles. CTX = cetuximab.

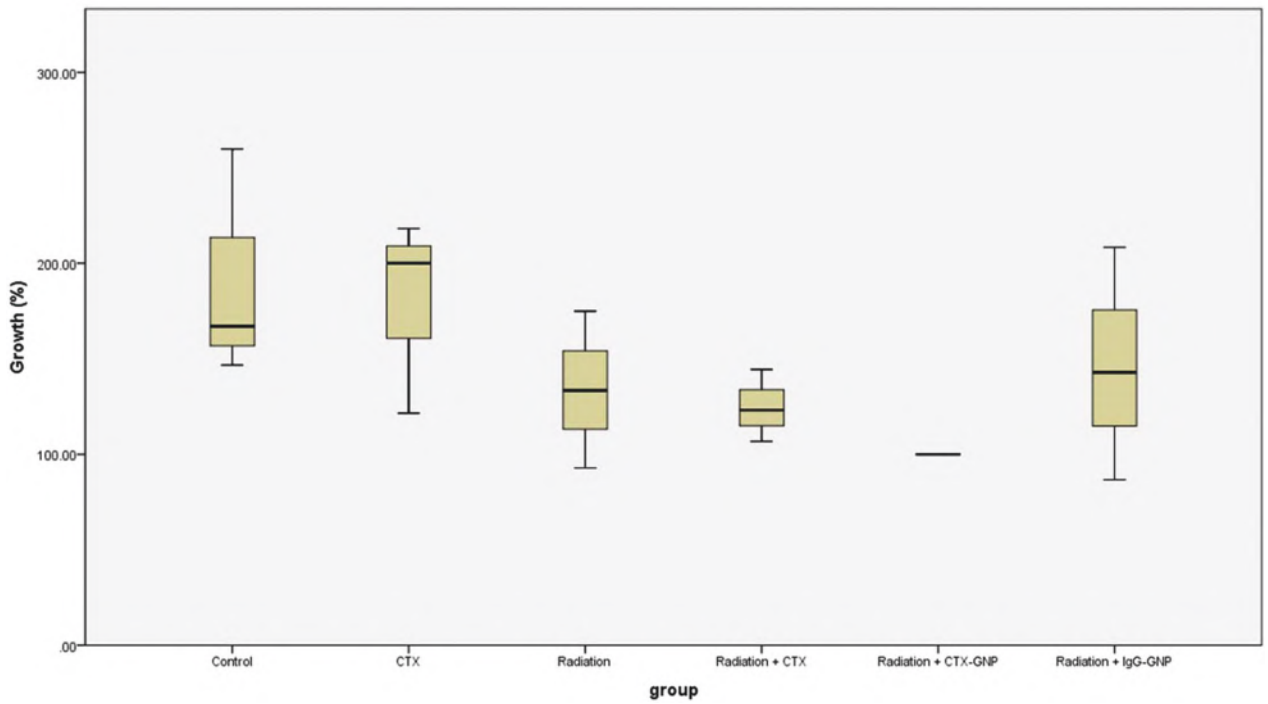

Fig. 4 Average changes in tumor growth per group.

1.9 cm; group 5: 1.3 to 1.9 cm; group 6: from 1.3 to 1.3 cm. The difference in tumor volume from the control group was statistically significant for the radiation + CTX-GNP group (P = 0.001), marginally significant for the radiation + CTX group (P = 0.055), and non-significant for the other groups (Fig. 3).

Biological mechanism of radiosensitizer-GNPs

The CD34 level was significantly lower at 1 and 6 weeks post treatment in the radiation + CTX-GNP group than the control, radiation-only, and radiation + CTX groups indicating decreased vascularization. Results of the TUNEL assay showed that compared to the radiation-only group, the radiation + CTX-GNP group displayed higher apoptosis at one week and less apoptosis at 6 weeks post treatment. PCNA and Ki-67 staining was weaker after both 1 and 6 weeks in the radiation + CTX-GNP group than in the other groups indicating a reduced level of proliferation and tissue repair (Fig. 5 and 6).

Toxicity

All mice remained alive to the end of the study except one control mouse that died after 5 weeks. None of the surviving mice showed a decline in well-being, as evaluated by food intake, weight, and behavior. No skin toxicity was detected.

Acute and late toxicity have been evaluated in six mice that received IV injection of CTX-GNP. The tests included well-being, hematological blood tests, kidney and liver functions

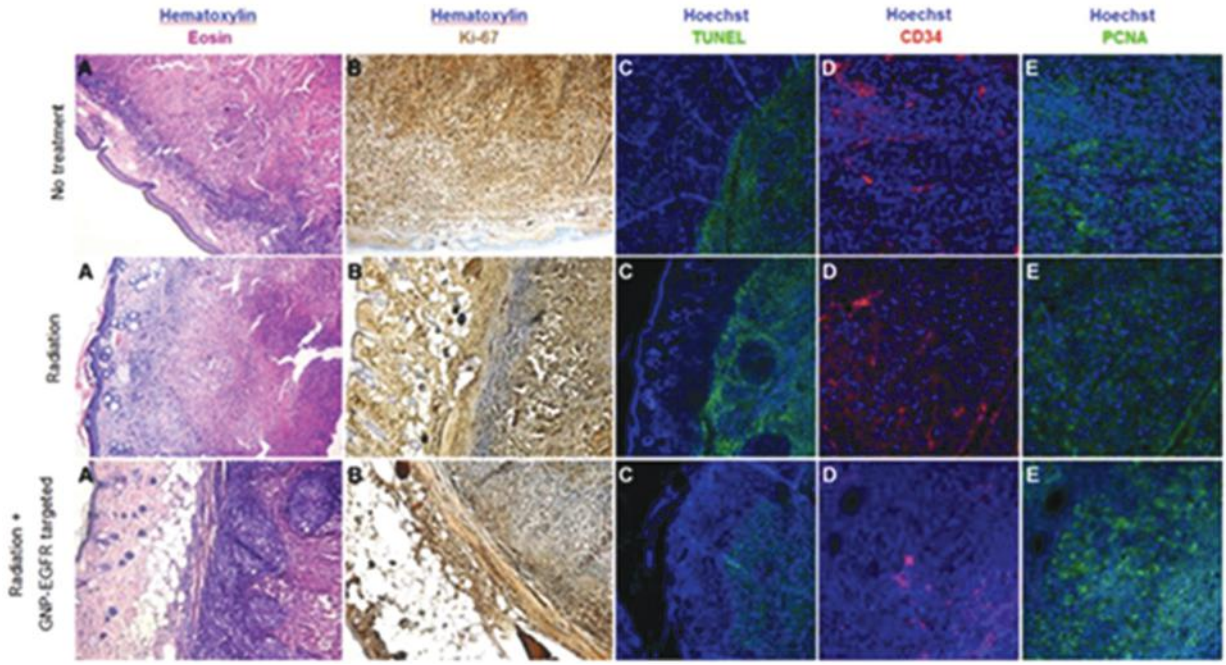

Fig. 5 Histological characterization 6 weeks post various treatments: representative images of tumor and adjacent tissue 6 weeks after saline (no treatment, A′–E′) administration, radiation only (A″–E″) and radiation + EGFR-GNP (A‴–E‴). Sections were stained with H&E (A′–A‴), Ki-67 (B′–B″, brown); TUNEL (C′–C‴, green), CD34 (D′–D‴, red) and PCNA (E′–E‴, green). Bar = 100 μm.

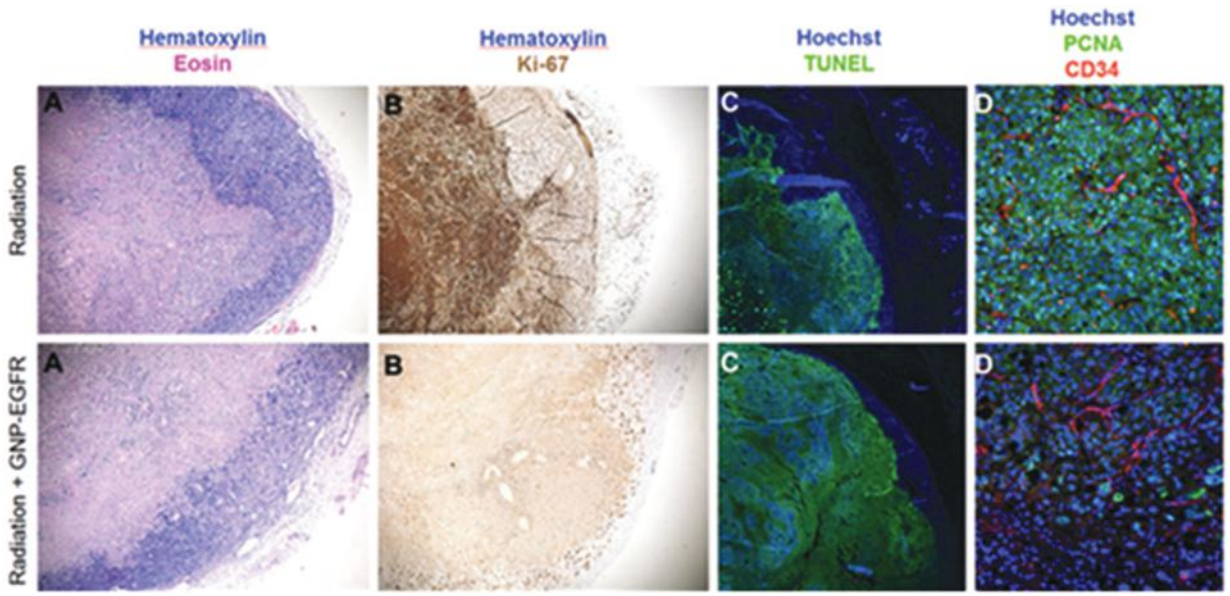

Fig. 6 Histological characterization 1 week post various treatments: representative images of tumor and adjacent tissue 1 week after radiation only (A′–D′) and radiation + EGFR-GNP (A″–D″). Sections were stained with H&E (A′–A″), Ki-67 (B′–B″, brown); TUNEL (C′–C″, green) and Hoechst (DNA, blue), CD34 and PCNA (D′–D″, red, green, respectively). ×10 magnification.

and biopsies. All six mice survived the full study period with no decline in well-being expressed by food intake, weight and normal behavior. There was no difference in blood count among the groups. No changes were noted in white blood cell hemoglobin or platelets during the study period and no significant changes in levels of creatinine or urea. A mild increase in liver transaminase levels was recorded in 2/6 mice tested at 4 weeks after injection of 6 mg CTX-GNP (Fig. 7).

Test	Unit	Pre-injection	One week post injection	Six weeks post injection
UREA	mg/dL	33.0	42.0	48.0
CRE	mg/dL	0.3	-0.1	0.0
ALB	g/dL	0.27	99	3.8
ALP	U/L	87	150	92
ALT	U/L	51	153	232
AST	U/L	135	3441	208
T. BIL	mg/dL	0.0	3.0	0.0

Fig. 7 Blood test results (median) before injection, and one week and six weeks after injection. CRE = creatinine, ALB = albumin, ALP = alkaline phosphatase, ALT = alanine aminotransferase, AST = aspartate aminotransferase, T. BIL = total bilirubin.

In order to evaluate possible pathological changes due to an increase in liver enzymes, histological examination of the liver and kidney (for the six mice) was performed (Fig. 8). The histological examination revealed that all but one showed mild–moderate hepatocellular hydropic degeneration indicating an accumulation of glycogen in the hepatocyte cytoplasm Fig. 8. These metabolic changes are typical of fasted animals held under stressful conditions and might explain the increase in serum liver transaminase levels. It is most likely not a cytotoxic effect. No changes were noted in the kidney in any of the mice evaluated.

Discussion

The use of targeted radiosensitizers in cancer treatment is intended to increase tumor sensitivity to radiation while sparing normal healthy tissue the effects of *x*-radiation, thereby increasing the therapeutic window. In the present study, we evaluated the effectiveness, biological mechanism and toxicity profile of targeted GNP (*via* CTX) followed by conventional 6 MV radiotherapy in HNSCC. The results showed that CTX-GNP injection was associated with a significant improvement in tumor radiosensitivity relative to the other modalities. However, the mechanism underlying cell death in GNP-induced radiation sensitivity is unclear and several theories have been proposed. Roa *et al.*[23] found that GNPs may sensitize radiotherapy by regulating the cell cycle. They showed that it induced the acceleration of the G0G1 phase and cell accumulation in the G2/M phase, which were accompanied by down-regulation of p53 and cyclin expression and upregulation of cyclin B1 and cyclin E. In the present study, TUNEL staining of the treated tumor at 1 week after treatment demonstrated enhanced and accelerated apoptosis compared to conventional radiation. Although Jain *et al.*[24] claimed that GNPs have no effect on the repair mechanism,

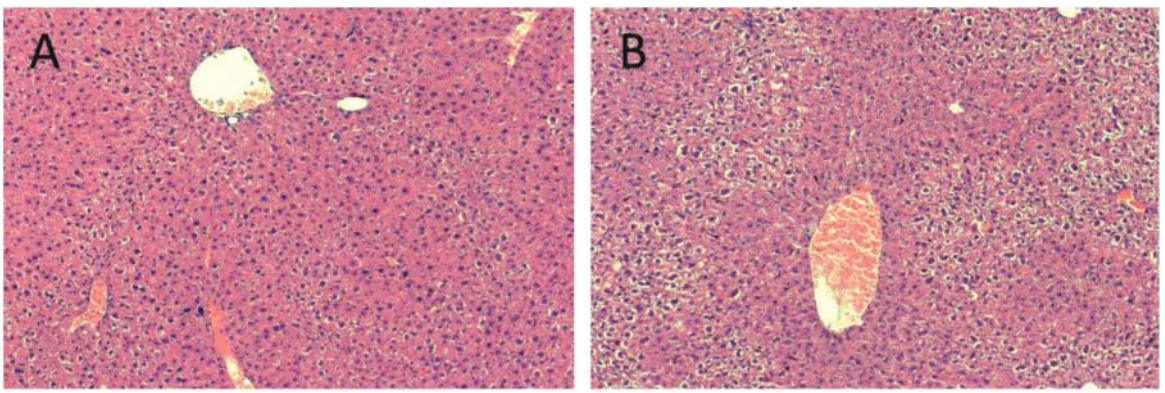

Fig. 8 Liver histology by hematoxylin and eosin (H&E) staining (magnification, ×40). A: Mild histological changes in liver tissue of mouse # 1. B: Moderate histological changes in liver tissue of mouse # 5. This hepatocellular hydropic degeneration is a common hepatic change in animals and most likely is not a cytotoxic effect.

PCNA staining after GNP treatment in the present study indicated lesser DNA repair over time. In addition, the significant change in CD34 staining pointed to an inhibition of angiogenesis. We can therefore conclude upon these immunohistological markers that GNP induced enhanced and earlier tumor apoptosis that is characterized by less vascularity and lower proliferation and tissue repair, thus implying a more efficient tumor eradication (Fig. 6).

No evidence of early or delayed toxicity has been observed. There was a mild increase in transaminase levels in 2 mice which may have been due to the stressful conditions (not toxicity) as indicated by histologic findings of hepatocellular hydropic degeneration. These findings suggest that a dose of 6 mg of GNP conjugated to CTX has low toxicity. In conclusion, this study describes a promising novel method to improve radiosensitivity and thereby patient survival in locally advanced HNSCC. Intravenous administration of GNP selectively targeted head and neck tumors and significantly increased the radiation absorbed in the tumor. The next step should include an evaluation of the effect of GNP on absorption of fractionated radiation and a phase Ib study, in which patients with recurrent radioresistant tumors will be treated.

Future perspective

We anticipate that this research will lay the groundwork for further fundamental research into the underlying mechanism whereby GNPs enhance the effect of radiation. This concept can be widely applied across multiple tumor types, leading to more effective clinical radiotherapy with less toxicity.

Conflicts of interest

There are no potential conflicts of interest.

Acknowledgements

This work was funded by a joint Rabin Medical Center and Bar-Ilan University grant.

References

1 D. Rischin, *et al.*, Tirapazamine, cisplatin, and radiation versus cisplatin and radiation for advanced squamous cell carcinoma of the head and neck (TROG 02.02, HeadSTART): a phase III trial of the Trans-Tasman Radiation Oncology Group, *J. Clin. Oncol.*, 2010, **28**, 2989–2995.
2 T. Reuveni, M. Motiei, Z. Romman, A. Popovtzer and R. Popovtzer, Targeted gold nanoparticles enable molecular CT imaging of cancer: an in vivo study, *Int. J. Nanomed.*, 2011, **6**, 2859–2864.
3 S.-D. Li and L. Huang, Pharmacokinetics and biodistribution of nanoparticles, *Mol. Pharm.*, 2008, **5**, 496–504.
4 C.-J. Liu, *et al.*, Enhancement of cell radiation sensitivity by pegylated gold nanoparticles, *Phys. Med. Biol.*, 2010, **55**, 931–945.
5 D. B. Chithrani, S. Jelveh, F. Jalali, M. van Prooijen, C. Allen, R. G. Bristow, R. P. Hill and D. A. Jaffray, *Radiat. Res.*, 2010, **173**, 719–728.
6 S. Jain, D. G. Hirst and J. M. O'Sullivan, Gold nanoparticles as novel agents for cancer therapy, *Br. J. Radiol.*, 2012, **85**, 101–113.
7 J. F. Hainfeld, D. N. Slatkin and H. M. Smilowitz, The use of gold nanoparticles to enhance radiotherapy in mice, *Phys. Med. Biol.*, 2004, **49**, N309–N315.
8 J. F. Hainfeld, *et al.*, Gold nanoparticles enhance the radiation therapy of a murine squamous cell carcinoma, *Phys. Med. Biol.*, 2010, **55**, 3045–3059.
9 E. Hebert, P. Debouttiere and D. Hunting, MRI detectable gadolinium-coated gold nanoparticles for radiotherapy, *Int. J. Radiat. Oncol., Biol., Phys.*, 2008, **72**, S715–716.
10 M.-Y. Chang, *et al.*, Increased apoptotic potential and dose-enhancing effect of gold nanoparticles in combination with single-dose clinical electron beams on tumor-bearing mice, *Cancer Sci.*, 2008, **99**, 1479–1484.
11 H. Haigler, J. F. Ash, S. J. Singer and S. Cohen, Visualization by fluorescence of the binding and internalization of epidermal growth factor in human carcinoma cells A-431, *Proc. Natl. Acad. Sci. U. S. A.*, 1978, **75**, 3317–3321.
12 J. R. Grandis, *et al.*, Levels of TGF- and EGFR protein in head and neck squamous cell carcinoma and patient survival, *JNCI, J. Natl. Cancer Inst.*, 1998, **90**, 824–832.
13 J. Baselga, The EGFR as a target for anticancer therapy—focus on cetuximab, *Eur. J. Cancer*, 2001, **37**, 16–22.
14 B. V. Enustun and J. Turkevich, Coagulation of colloidal gold, *J. Am. Chem. Soc.*, 1963, **85**, 3317–3328.
15 S. Moghimi, A. Hunter and J. Murray, Long-circulating and target-specific nanoparticles: theory to practice, *Pharmacol. Rev.*, 2001, **53**(2), 283–318.
16 X. Qian, *et al.*, In vivo tumor targeting and spectroscopic detection with surface-enhanced Raman nanoparticle tags, *Nat. Biotechnol.*, 2008, **26**, 83–90.
17 X. Wang, *et al.*, Detection of circulating tumor cells in human peripheral blood using surface-enhanced Raman scattering nanoparticles, *Cancer Res.*, 2011, **71**, 1526–1532.
18 J. F. Hainfeld, D. N. Slatkin, T. M. Focella and H. M. Smilowitz, Gold nanoparticles: a new X-ray contrast agent, *Br. J. Radiol.*, 2006, **79**, 248–253.
19 J. F. Hainfeld, D. N. Slatkin and H. M. Smilowitz, The use of gold nanoparticles to enhance radiotherapy in mice, *Phys. Med. Biol.*, 2004, **49**(18), N309–N315.
20 W. H. De Jong, *et al.*, Particle size-dependent organ distribution of gold nanoparticles after intravenous administration, *Biomaterials*, 2008, **29**, 1912–1919.
21 J. Hainfeld and F. Dilmanian, Radiotherapy enhancement with gold nanoparticles, *J. Pharm. Pharmacol.*, 2008, **60**(8), 977–985.
22 R. Wild, K. Fager, C. Flefleh and D. Kan, Cetuximab preclinical antitumor activity (monotherapy and combination

based) is not predicted by relative total or activated epidermal growth factor receptor tumor, *Mol. Cancer Ther.*, 2006, available at http://mct.aacrjournals.org/content/5/1/104.short.

23 W. Roa, X. Zhang, L. Guo, A. Shaw and X. Hu, Gold nanoparticle sensitize radiotherapy of prostate cancer cells by regulation of the cell cycle, *Nanotechnology*, 2009, **20**, 375101.

24 S. Jain, J. Coulter and A. Hounsell, Cell-specific radiosensitization by gold nanoparticles at megavoltage radiation energies, *Int. J. Radiat. Oncol. Biol. Phys.*, 2011, **79**(2), 531–539.

